Low-Temperature Single-Wall Carbon Nanotube Synthesis by Thermal Chemical Vapor Deposition

Hongwei Liao[†] and Jason H. Hafner*[,†,‡]

Department of Chemistry, and Department of Physics and Astronomy, Rice University, 6100 Main Street, Houston, Texas 77005

Received: April 1, 2004; In Final Form: April 27, 2004

Reduced-temperature synthesis of single-wall carbon nanotubes (SWNTs) is of interest for their growth into device architectures and their efficient bulk production. SWNTs were grown via the thermal chemical vapor deposition (CVD) of low-pressure ethylene over iron particles supported on silicon wafers at temperatures down to 550 °C. The SWNT structure and quality were confirmed by atomic force microscopy (AFM) and micro-Raman spectroscopy.

Introduction

Because of their outstanding mechanical, electronic, and chemical properties, single-wall carbon nanotubes (SWNTs) have been intensely studied, and promising applications have been demonstrated.[1] Although SWNTs have been synthesized by several different processes, the most versatile is chemical vapor deposition (CVD), in which preformed nanometer-scale catalyst particles supported on surfaces are heated to 700−1000 °C in an atmosphere containing either a hydrocarbon[2] or carbon monoxide.[3] Two potential SWNT application areas indicate the need for SWNT synthesis at reduced temperatures. The first is the growth of SWNTs directly into device architectures. Electrodes have been applied to surface-bound SWNTs with nanolithography to create devices such as nanometer-scale field-effect transistors[4] and chemical sensors.[5] A more scalable procedure is to grow SWNTs directly into preformed electrode patterns; however, the high growth temperatures are usually destructive. Although devices have been formed with refractory molybdenum interconnects for greater stability,[6] a more productive route would be to reduce the SWNT synthesis temperature to make it compatible with a wider range of substrates and nanofabrication technology. The second area is the need for efficient synthesis. When performed in the gas phase, CVD can produce SWNTs in gram quantities, which is sufficient for basic research and to demonstrate bulk applications.[7] For example, SWNTs have been spun into fibers whose properties suggest applications such as strong, tough materials and supercapacitors.[8,9] However, further applications development will require much more material at a greatly reduced cost per gram. Lower-temperature synthesis is one of many advances needed to achieve the goal of inexpensive, plentiful SWNTs. Three groups have reported thermal CVD synthesis down to 680 °C,[10,11] 650 °C,[12] and 600 °C[13] and explicitly demonstrated a strong lower limit to the synthesis temperature. Plasma-enhanced CVD and hot-wire CVD can reduce the supporting substrate temperature to 550 °C[14] and 450 °C,[15] respectively; however, these methods do not fully address the needs of the applications described previously. In addition, plasma enhancement has recently been shown to heat the substrate significantly.[16]

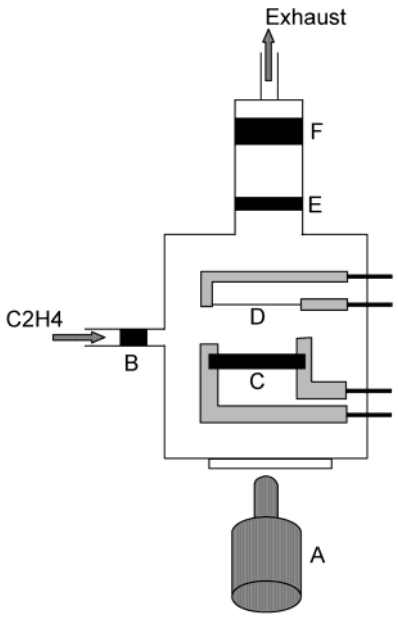

Figure 1. Schematic of the low-pressure chemical vapor deposition single-walled carbon nanotube (CVD SWNT) synthesis apparatus. Legend is as follows: A, IR pyrometer; B, mass flow controller; C, silicon substrate, D, iron wire; E, throttle valve, and F, turbopump.

Experimental Section

We have built a turbo-pumped low-pressure CVD reactor that provides precise and rapid control of SWNT synthesis conditions, to study the mechanisms of SWNT nucleation and growth microscopically. In the reactor (Figure 1), *n*-doped silicon substrates (30 mm × 2 mm chips, $R < 0.004\ \Omega$ cm) are resistively heated and their temperature monitored by an IR pyrometer (model Modline 3, IRCON). The pyrometer is centered on a reference mark on the wafer surface to identify the location of the temperature measurement. Ethylene is admitted through mass flow controllers (model 1179A, MKS Instruments), and its pressure is controlled by a downstream throttle valve (model 653B, MKS Instruments). With this setup, the controllable substrate temperature range is 550−800 °C, and the controllable ethylene pressure range is 1−500 mTorr at flow rates of 0.1−1 SCCM (standard cubic centimeter per minute).

[†] Department of Chemistry.
[‡] Department of Physics and Astronomy.

10.1021/jp048566n CCC: $27.50
Published on Web 05/12/2004

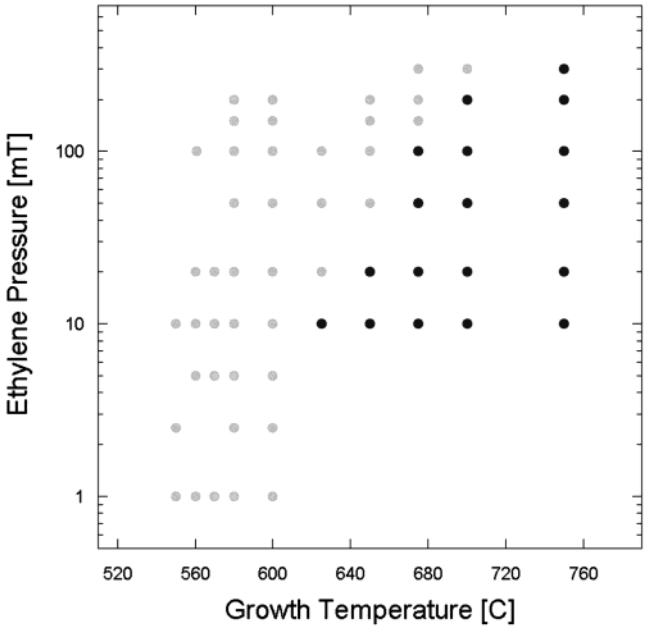

Figure 2. SWNT synthesis phase space. All experiments were performed under identical catalyst preparation conditions and growth times of 500 s. Gray circles represent ethylene pressures and substrate temperatures for which nanotubes were found by AFM, and black circles represent conditions for which they were not.

The base pressure is 10^{-6} Torr. Submonolayer coverage of a catalyst is deposited onto the silicon substrate under high vacuum by a resistively heated 5-mil-diameter iron wire ~3 cm away. At elevated substrate temperatures, the surface-bound iron species become mobile and coalesce to form catalyst particles 1−3 nm in diameter on the silicon wafer.[17] For SWNT nucleation and growth, ethylene is admitted to the turbo-pumped chamber at 1−100 mTorr and the substrate is heated to the growth temperature. After synthesis, the substrates are analyzed by atomic force microscopy (AFM) (Nanoscope IV Multimode AFM, Veeco Metrology) and resonant micro-Raman spectroscopy with 633 nm excitation (Ramanscope, Renishaw). Regions for analysis by AFM and micro-Raman spectroscopy are randomly chosen within 1 mm of the center of the reference mark. For AFM, several 2 μm × 2 μm scans are acquired to determine if nanotubes are present. Similar results were always observed anywhere in the region of controlled temperature.

Results and Discussion

As an initial step in studying the kinetics of SWNT synthesis, we have mapped the synthesis "phase space" for this system (Figure 2). Surprisingly, we find that, at pressures of 10 mTorr of ethylene or less, SWNT synthesis (possibly including some double-wall nanotubes)[18] occurs down to a growth temperature of 550 °C, which is significantly below previous reports on thermal CVD SWNT synthesis.[10−13] Note that this lower limit is imposed by the IR pyrometer, and that it is possible that SWNTs will grow at even lower temperatures under these conditions. One must be cautious when using pyrometry for absolute temperature measurements of small objects. To test the validity of the temperature measurements, identical silicon chips were placed in a quartz tube furnace at typical growth temperatures. Comparisons of the pyrometric measurements and furnace temperatures were within 10 °C. Figure 3a−d displays AFM images of SWNT synthesized at 550 °C and 10 mTorr of ethylene. Nanotubes and unsuccessful catalyst particles are clearly visible. Nanotube diameters were measured by AFM,

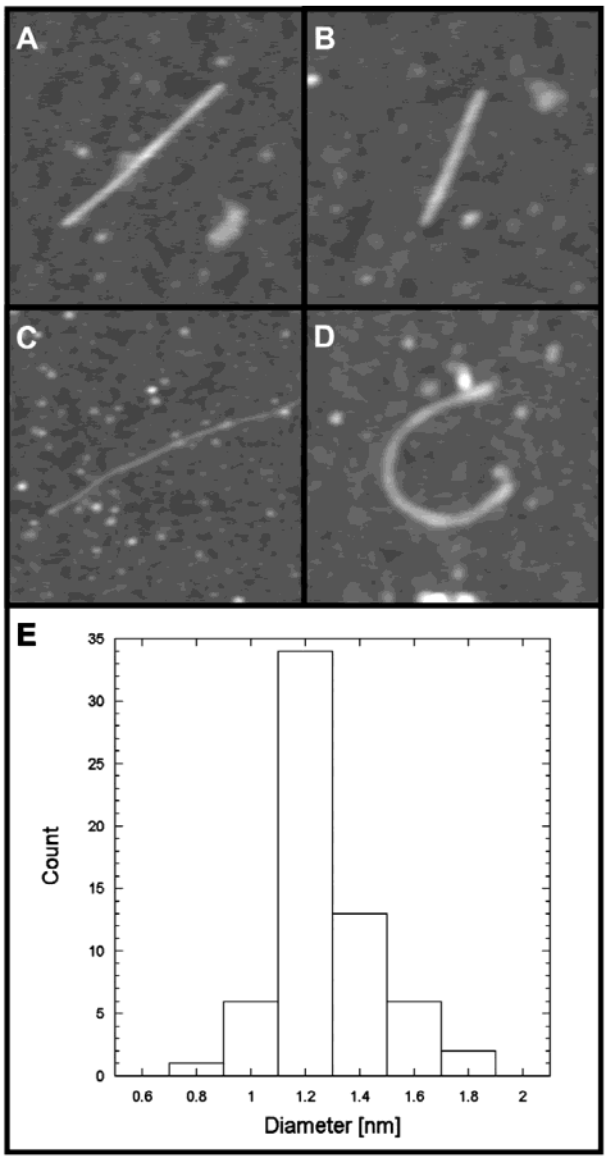

Figure 3. (A−D) AFM micrographs (250 nm × 250 nm, 5-nm linear gray scale in *z*) of individual catalyst particles and SWNT synthesized at 550 °C in 10 mTorr of ethylene for 500 s. The diameter distribution in panel E was taken from AFM measurements of the heights of 62 different nanotubes.

revealing the fairly narrow size distribution plotted in Figure 3e. Nanotube yields (defined as the number of nanotubes divided by the total number of catalyst particles) were on the order of 0.1%−10%. The yield increased approximately with pressure and was approximately independent of temperature; however, it was also highly dependent on the catalyst particle size and density. Because the catalyst particle properties were not well-controlled, we cannot draw any quantitative conclusions on the pressure and temperature dependence of nucleation, and we are currently reporting only the presence or lack of nanotubes in Figure 2.

Although the pyrometer cannot measure at temperatures <550 °C for small samples, we attempted to study SWNT synthesis below this level to find the low-temperature limit. The substrate temperature is controlled by a feedback loop between the heating power supply and the pyrometer. The substrate temperature was plotted as a function of the steady-state heating power. This plot was extrapolated to lower temperatures, and the system was operated at constant power for growth experiments in the 500−550 °C range. We typically found that, under constant

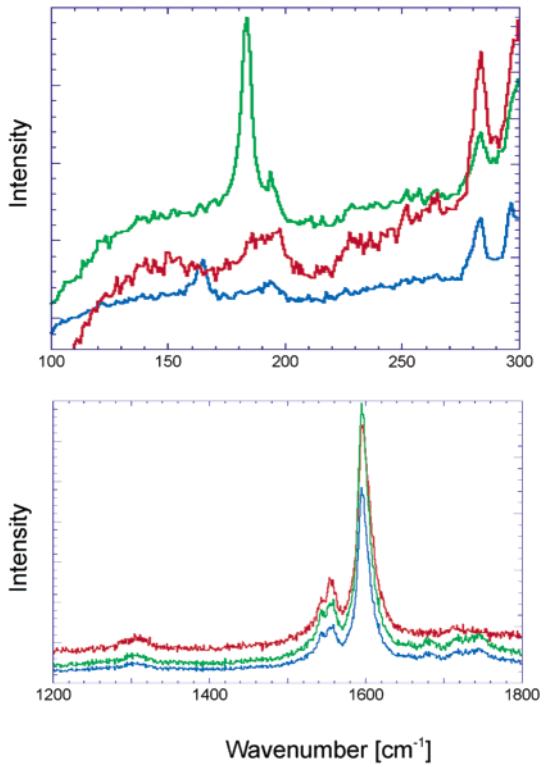

Figure 4. Resonant micro-Raman spectra of three positions on a silicon wafer with SWNT synthesized at 560 °C. The top graph shows RBM peaks at 150−300 cm^{-1}, and the bottom graph shows both D- (1310 cm^{-1}) and G(1580 cm^{-1})-bands.

power operation, the temperature would drift upward by 10 °C over the course of the experiment. From these measurements and growth experiments, we estimate the lower temperature limit of SWNT synthesis to be in the range of 530−540 °C.

A significant fraction of the nanotubes are curved with a radius of ∼50 nm, as in Figure 3d. This structural feature could suggest that they are defective because of the reduced synthesis temperature. To assess the SWNT structure and quality further, the samples were analyzed by resonant micro-Raman spectroscopy (Figure 4), in which Raman spectra are collected from a single or a few SWNTs in a highly focused laser beam spot. The peaks between 150 and 300 cm^{-1} represent the SWNT radial breathing modes (RBMs). The 303 cm^{-1} peak due to the silicon substrate is cut off in the graph, but its edge is apparent. Using the approximate expression $d_{SWNT}(nm) = 248/\omega_{RBM}(cm^{-1})$,[19] we find that the two groups of RBM peaks correspond to nanotubes with diameters of ∼1.4 and ∼0.9 nm. These measurements are consistent with the diameter distribution determined by AFM. The apparent diameter gap in the micro-Raman measurements is due to the resonance condition between the laser and the SWNT van Hove singularities. The 1.96 eV laser wavelength is resonant with the E_{11} transition for the metallic SWNT in the small-diameter portion of the distribution and the E_{22} transition of the semiconductors with larger diameter. The tangential G-band and disorder-related D-band were also observed for each spot that contained an RBM peak. The narrow width of the G-band, the weak signal in the D-band,[10] and the general similarity of these Raman spectra to those of SWNTs synthesized at higher temperatures[20] suggest that at least some fraction of these SWNTs is not highly disordered.

Although SWNT nucleation and growth are not well understood, they are thought to result from the following reactions: precursor decomposition on the catalyst particle surface, carbon diffusion across the catalyst particle, and carbon addition to a SWNT (growth) or nucleation of a SWNT (nucleation).[21] The reduced synthesis temperature observed here could simply be due to the lower stability of the ethylene precursor relative to methane and carbon monoxide, which are more widely used for SWNT synthesis by thermal CVD. This would imply that the lower temperature limit is set by the precursor decomposition step, and that even lower SWNT synthesis temperatures could be achieved with less-stable precursors. In support of this view, CVD-produced carbon nanofibers that are thought to grow by similar reaction mechanisms are synthesized down to 500 °C.[22] However, the picture is likely to be more complicated than simply an effect of precursor stability. Figure 2 clearly shows that, at some temperatures, nucleation and growth are also dependent on pressure. Future studies will explore this issue and the lower-temperature limits of SWNT synthesis.

Acknowledgment. This work was supported by the Robert A. Welch Foundation, the ACS Petroleum Research Fund, and Rice University.

References and Notes

(1) Baughman, R. H.; Zakhidov, A. A.; de Heer, W. A. *Science* **2002**, *297*, 787−792.

(2) Kong, J.; Soh, H. T.; Cassell, A. M.; Quate, C. F.; Dai, H. *Nature* **1998**, *395*, 878−881.

(3) Zheng, B.; Lu, C.; Gu, G.; Makarovski, A.; Finkelstein, G.; Liu, J. *Nano Lett.* **2002**, *2*, 895−898.

(4) Tans, S. J.; Verschueren, A. R. M.; Dekker, C. *Nature* **1998**, *393*, 49−52.

(5) Dai, H. J. *Acc. Chem. Res.* **2002**, *35*, 1035−1044.

(6) Franklin, N. R.; Wang, Q.; Tombler, T. W.; Javey, A.; Shim, M.; Dai, H. *Appl. Phys. Lett.* **2002**, *81*, 913−915.

(7) Nikolaev, P.; Bronikowski, M. J.; Bradley, R. K.; Rohmund, F.; Colbert, D. T.; Smith, K. A.; Smalley, R. E. *Chem. Phys. Lett.* **1999**, *313*, 91−97.

(8) Dalton, A. B.; Collins, S.; Munoz, E.; Razal, J. M.; Ebron, V. H.; Ferraris, J. P.; Coleman, J. N.; Kim, B. G.; Baughman, R. H. *Nature* **2003**, *423*, 1888−1893.

(9) Davis, V. A.; Ericson, L. M.; Parra-Vasquez, A. N. G.; Fan, H.; Wang, Y.; Prieto, V.; Longoria, J. A.; Ramesh, S.; Saini, R. K.; Kittrell, C.; Billups, W. E.; Adams, W. W.; Hauge, R. H.; Smalley, R. E.; Pasquali, M. *Macromolecules* **2004**, *37*, 154−160.

(10) Harutyunyan, A. R.; Pradhan, B. K.; Kim, U. J.; Chen, G.; Eklund, P. C. *Nano Lett.* **2002**, *2*, 525−530.

(11) Hornyak, G. L.; Grigorian, L.; Dillon, A. C.; Parilla, P. A.; Jones, K. M.; Heben, M. J. *J. Phys. Chem. B* **2002**, *106*, 2821−2825.

(12) Hongo, H.; Nihey, F.; Ichihashi, T.; Ochiai, Y.; Yudasaka, M.; Iijima, S. *Chem. Phys. Lett.* **2003**, *380*, 158−164.

(13) Seidel, R.; Duesberg, G. D.; Unger, E.; Graham, A. P.; Liebau, M.; Kreupl, F. *J. Phys. Chem. B* **2004**, *108*, 1888.

(14) Kato, T.; Jeong, G.; Hirata, T.; Hatakeyama, R.; Tohji, K.; Motomiya, K. *Chem. Phys. Lett.* **2003**, *381*, 422−426.

(15) Mahan, A. H.; Alleman, J. L.; Heben, M. J.; Parilla, P. A.; Jones, K. M.; Dillon, A. C. *Appl. Phys. Lett.* **2002**, *81*, 4061−4063.

(16) Teo, K. B. K.; Hash, D. B.; Lacerda, R. G.; Rupesinghe, N. L.; Bell, M. S.; Dalal, S. H.; Bose, D.; Govindan, T. R.; Cruden, B. A.; Chhowalla, M.; Amaratunga, G. A. J.; Meyyappan, M.; Milne, W. I. *Nano Lett.* **2004**, *4*, 921−926.

(17) Berko, A.; Klivenyi, G.; Solymosi, F. *J. Catal.* **1999**, *182*, 511−514.

(18) Hafner, J. H.; Bronikowski, M. J.; Azamian, B. R.; Nikolaev, P.; Rinzler, A. G.; Colbert, D. T.; Smith, K. A.; Smalley, R. E. *Chem. Phys. Lett.* **1998**, *296*, 195−202.

(19) Jorio, A.; Raito, R.; Hafner, J. H.; Lieber, C. M.; Hunter, M.; McClure, T.; Dresselhaus, G.; Dresselhaus, M. S. *Phys. Rev. Lett.* **2001**, *86*, 1118−1121.

(20) Dresselhaus, M. S.; Dresselhaus, G.; Jorio, A.; Souza Filho, A. G.; Saito, R. *Carbon* **2002**, *40*, 2043−2061.

(21) Dai, H. J.; Rinzler, A. G.; Nikolaev, P.; Thess, A.; Colbert, D. T.; Smalley, R. E. *Chem. Phys. Lett.* **1996**, *260*, 471−475.

(22) Rodriguez, N. M. *J. Mater. Res.* **1993**, *8*, 3233−3250.